DALTON

Synthesis, structures and redox properties of platinum metal phosphathia complexes: crystal structures of *cis*-$[RuCl_2(RSC_2H_4SR)]\cdot0.75Et_2O$ and *cis*-$[RhCl_2(RSC_2H_4RS)]PF_6\cdot CH_2Cl_2$ (R = $Ph_2PCH_2CH_2$)

Neil R. Champness,[a] **Robin J. Forder,**[a] **Christopher S. Frampton**[b] **and Gillian Reid** *[,a]

[a] *Department of Chemistry, University of Southampton, Highfield, Southampton SO17 1BJ, UK*
[b] *Roche Products Ltd., Welwyn Garden City, Hertfordshire AL7 3AY, UK*

Reaction of $[RuCl_2(py)_4]$ (py = pyridine) with 1 molar equivalent of the new tetradentate acyclic phosphathia compound RSC_2H_4SR ($Ph_2PCH_2CH_2SCH_2CH_2SCH_2CH_2PPh_2$) or the macrocycle *meso*-$Ph_2[14]aneP_2S_2$ (4,8-diphenyl-1,11-dithia-4,18-diphosphacyclotetradecane) in refluxing toluene under a nitrogen atmosphere afforded the ruthenium(II) complexes $[RuCl_2(RSC_2H_4SR)]$ and $[RuCl_2(Ph_2[14]aneP_2S_2)]$ respectively as yellow solids. The crystal structure of $[RuCl_2(RSC_2H_4SR)]\cdot0.75Et_2O$ shows RSC_2H_4SR co-ordinated *via* all four donor atoms with the two P-donors occupying mutually *trans* co-ordination sites at Ru^{II}, and *cis*-dichlorides completing the overall octahedral stereochemistry, Ru–S 2.294(1), 2.292(1), Ru–P 2.339(2), 2.335(2), Ru–Cl 2.463(1), 2.463(1) Å. Phosphorus-31 NMR spectroscopic studies on the macrocyclic species $[RuCl_2(Ph_2[14]aneP_2S_2)]$ are consistent with a *cis*-dichloro isomer in which one Cl is *trans* to P and the other *trans* to S. Cyclic voltammetry showed a reversible one-electron oxidation occurring at $E_{\frac{1}{2}} = +0.16$ and $+0.32$ V *vs.* ferrocene–ferrocenium for $[RuCl_2(RSC_2H_4SR)]$ and $[RuCl_2(Ph_2[14]aneP_2S_2)]$ respectively. The complexes $[MCl_2(RSC_2H_4SR)]PF_6$ (M = Rh or Ir) have also been prepared. The structure of $[RhCl_2(RSC_2H_4SR)]PF_6\cdot CH_2Cl_2$ shows discrete $[RhCl_2(RSC_2H_4SR)]^+$ cations adopting a very similar arrangement to that in the ruthenium(II) analogue, with Rh–P 2.352(2), 2.342(2), Rh–S 2.303(2), 2.297(2), Rh–Cl 2.370(2), 2.359(2) Å. Rhodium-103 NMR spectroscopy reveals a triplet at δ +1405 (J_{RhP} 85 Hz).

Acyclic phosphine ligands are well known to form stable complexes with many metal ions,[1] whereas acyclic thioether complexes tend to be less stable, and often hydrolyse readily.[2] Macrocyclic thioethers, on the other hand, form complexes which are often significantly more robust with respect to demetallation.[3] As part of a long-term project probing the differences in reactivity between phosphine ligands which involve cyclic *vs.* acyclic arrangements, we have been looking at ways of incorporating phosphine functions into macrocyclic environments and comparing the chemistry of these new macrocyclic compounds with that of related acyclic ligands which possess similar donor sets. We have recently reported the synthesis of the mixed phosphathia macrocycle $Ph_2[14]aneP_2S_2$ (4,8-diphenyl-1,11-dithia-4,8-diphosphacyclotetradecane), together with its complexes of Pd^{II}, Pt^{II} and Rh^{III}.[4] Specifically, the acyclic phosphathia ligands which we have chosen to study in parallel incorporate the phosphine functions at the termini, with the thioether functions internal to the chain. We anticipated that, as phosphines are better σ donors compared to thioethers, this would assist in stabilisation of the mixed phosphine-thioether co-ordination, inhibiting decomplexation of the more weakly bound thioethers in solution. The copper(I) complex $[Cu(RSC_2H_4SR)]^+$ (R = $Ph_2PC_2H_4$) shows tetrahedral ligation *via* a P_2S_2-donor set,[5] while the gold(I) complexes $[AuL]PF_6$ (L = RSC_2H_4SR or RSC_3H_6SR) on the other hand adopt geometries intermediate between linear (P_2) and tetrahedral (P_2S_2), involving long-range, weak Au···S interactions of *ca.* 3 Å.[6] This paper describes the synthesis, spectroscopic characterisation and redox properties of $[RuCl_2(RSC_2H_4SR)]$, $[MCl_2(RSC_2H_4SR)]PF_6$ (M = Ir or Rh) and the macrocyclic species $[RuCl_2(Ph_2[14]aneP_2S_2)]$. We are not aware of any other examples of ruthenium complexes involving phosphine or phosphathia macrocycles. Single-crystal structure determinations on $[RuCl_2(RSC_2H_4SR)]\cdot$ $0.75Et_2O$ and $[RhCl_2(RSC_2H_4SR)]PF_6\cdot CH_2Cl_2$ are also reported.

RSC_2H_4SR

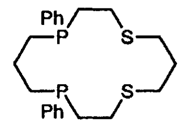

$Ph_2[14]aneP_2S_2$

Results and Discussion

Reaction of $[RuCl_2(py)_4]$ (py = pyridine) with 1 molar equivalent of *meso*-$Ph_2[14]aneP_2S_2$ in refluxing toluene under a nitrogen atmosphere gave a yellow solution. Upon cooling a yellow solid was deposited which was filtered off and recrystallised from CH_2Cl_2–diethyl ether. The FAB mass spectrum (3-nitrobenzyl alcohol matrix) shows peaks at *m*/*z* = 557, 521 and 446, with the correct isotopic distributions for $[^{102}Ru^{35}Cl(Ph_2[14]aneP_2S_2)]^+$, $[^{102}Ru(Ph_2[14]aneP_2S_2 - H)]^+$ and $[^{102}Ru(Ph[14]aneP_2S_2 + H)]^+$ respectively. The IR spectrum (CsI disc) shows two peaks at 309 and 283 cm^{-1} assigned to ν(Ru–Cl). Phosphorus-31 NMR spectroscopy (145.8 MHz, CH_2Cl_2–$CDCl_3$) shows a pair of doublets at δ + 63.5 and +54.7 ($^2J_{PP}$ = 40 Hz), indicative of a *cis*-dichloro stereochemistry. These signals are shifted downfield of free *meso*-$Ph_2[14]aneP_2S_2$ by some 80–90 ppm, diagnostic of formation of a five-membered chelate ring at each P-donor and thus confirming that in addition to the phosphines the thioether functions are also co-ordinated in solution.[7] These results, together with ^1H NMR, UV/VIS spectroscopic and microanalytical data, strongly support the formulation *cis*-$[RuCl_2(Ph_2[14]aneP_2S_2)]$ for this product, in which one phosphine donor occupies a site *trans* to S while the other lies *trans* to Cl$^-$, as illustrated in Fig. 1.

The *cis*-dichloro stereochemistry proposed for [RuCl$_2$(Ph$_2$[14]aneP$_2$S$_2$)] contrasts with the structure which we reported previously for the rhodium(III) cationic species [RhCl$_2$(Ph$_2$[14]aneP$_2$S$_2$)]$^+$ in which a *trans* dichloride arrangement is observed in the solid state by X-ray crystallography and in solution by ^{31}P NMR spectroscopy.[4] This difference is presumably principally a consequence of the slightly larger ionic radius for Ru^{II} *vs.* Rh^{III} (*ca.* 0.74 and 0.665 Å respectively),[8,*] and illustrates a fine balance between the constraints of the cavity size available for Ph$_2$[14]aneP$_2$S$_2$ and the strain imparted particularly by the phenyl rings on the P-donors on a folded form of *meso*-Ph$_2$[14]aneP$_2$S$_2$. Indeed, we commented previously that the related tetrathioether macrocyclic species [RhCl$_2$([14]aneS$_4$)]$^+$,[9] [IrCl$_2$([14]aneS$_4$)]$^+$[10] and [RuCl$_2$([14]aneS$_4$)][11] ([14]aneS$_4$ = 1,4,8,11-tetrathiacyclotetradecane) all adopt *cis* arrangements of the Cl$^-$ ligands with the macrocycle in a folded conformation.

We have also investigated the co-ordination chemistry of the related acyclic P$_2$S$_2$ donor RSC$_2$H$_4$SR (Ph$_2$PCH$_2$CH$_2$SCH$_2$CH$_2$SCH$_2$CH$_2$PPh$_2$) in which the P donors are located at the termini of the chain. We anticipated that placing the better σ donors at the termini would render the resultant complexes more stable with respect to demetallation. This open-chain compound was prepared by modification of a literature method.[12] Thus, PPh$_2$H was treated first with LiBu^n in dry, degassed tetrahydrofuran (thf) solution, followed by 1 molar equivalent of $\overline{SCH_2C}H_2$. Addition of 0.5 molar equivalents of BrCH$_2$CH$_2$Br to the resulting yellow solution, followed by hydrolysis, extraction (diethyl ether) and recrystallisation from CH$_2$Cl$_2$–diethyl ether gave RSC$_2$H$_4$SR as a white solid (^{31}P NMR δ −16.3; FAB mass spectrum *m/z* = 519, [RSC$_2$H$_4$SR + H]$^+$).

The compound RSC$_2$H$_4$SR, reacts with 1 molar equivalent of [RuCl$_2$(py)$_4$] in refluxing degassed toluene to afford an orange air-stable solid which was filtered off and recrystallised from CH$_2$Cl$_2$–diethyl ether. The FAB mass spectrum shows molecular ion peaks at *m/z* = 690, 655 and 627 with the correct isotopic distributions for [^{102}Ru^{35}Cl$_2$(RSC$_2$H$_4$SR)]$^+$, [^{102}Ru^{35}Cl(RSC$_2$H$_4$SR)]$^+$ and [^{102}Ru^{35}Cl(RSC$_2$H$_4$SR − C$_2$H$_4$)]$^+$ respectively. These data, together with ^{1}H NMR, UV/VIS spectroscopic and microanalytical data, confirm the formulation [RuCl$_2$(RSC$_2$H$_4$SR)]. The ^{31}P NMR spectrum (145.8 MHz, CDCl$_3$) shows a singlet at δ +42.7 confirming a single isomeric form in solution. Again, the large downfield shift relative to free RSC$_2$H$_4$SR is indicative of a five-membered chelate ring at each P-donor and hence strong evidence that the thioether functions are co-ordinated in solution.[7] Upon co-ordination of linear tetradentate RSC$_2$H$_4$SR to a six-co-ordinate metal ion several isomeric forms are possible.[13] Specifically, the equivalence of the phosphine suggests that the complex adopts either a *trans* or *cis*- α form. Unambiguous assignment of Ru–Cl stretches in the IR spectrum of [RuCl$_2$(RSC$_2$H$_4$SR)] was not possible.

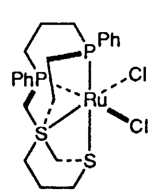

Fig. 1 Proposed structure of [RuCl$_2$(Ph$_2$[14]aneP$_2$S$_2$)]

In order to confirm the stereochemistry around the Ru^{II} ion a single-crystal structure determination of [RuCl$_2$(RSC$_2$H$_4$SR)]·0.75Et$_2$O was undertaken. This shows (Fig. 2, Table 1) the Ru^{II} co-ordinated to all four donor atoms of the phosphathia ligand with *cis*-dichloride ligands completing a distorted-octahedral stereochemistry. Consistent with the solution ^{31}P NMR data, the P-donors occupy mutually *trans* co-ordination sites in the crystalline form and hence are equivalent, with the ligand in the *cis*-α form, Ru–P(1) 2.339(2), Ru–P(2) 2.335(2), Ru–S(1) 2.294(1), Ru–S(2) 2.292(1), Ru–Cl(1) 2.463(1) and Ru–Cl(2) 2.463(1) Å. Notably, the trend observed in the bond distances around the Ru^{II} (*i.e.* Ru–S < Ru–P < Ru–Cl) differs from that in *trans*-[RhCl$_2$(Ph$_2$[14]aneP$_2$S$_2$)]$^+$ (*i.e.* Rh–P < Rh–S < Rh–Cl), presumably due to the *trans* influence of the Cl$^-$ ligands upon the metal–thioether bonding. The *cis* angles around the Ru lie in the range 85.6–94.2°; those involved in five-membered chelate rings are all less than 90°, reflecting the restricted bite size of the PCH$_2$CH$_2$S and SCH$_2$CH$_2$S linkages. It is noticeable that the particular co-ordination mode

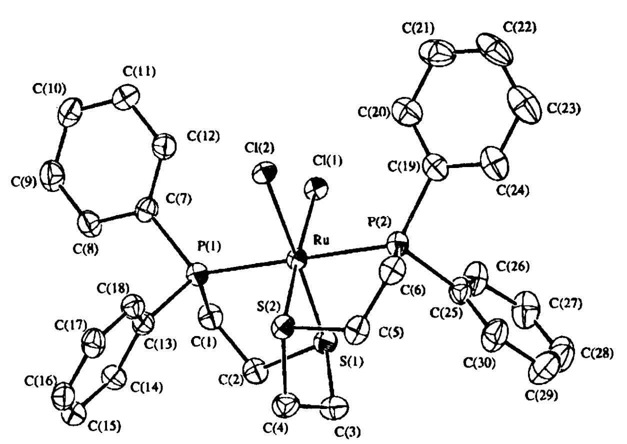

Fig. 2 View of the structure of *cis*-[RuCl$_2$(RSC$_2$H$_4$SR)] with the numbering scheme adopted; H atoms are omitted for clarity

Table 1 Selected bond lengths (Å) and angles (°) for *cis*-[RuCl$_2$(RSC$_2$H$_4$SR)]

Ru–Cl(1)	2.463(1)	Ru–Cl(2)	2.463(1)
Ru–S(1)	2.294(1)	Ru–S(2)	2.292(1)
Ru–P(1)	2.339(2)	Ru–P(2)	2.335(2)
S(1)–C(2)	1.846(5)	S(1)–C(3)	1.822(5)
S(2)–C(4)	1.825(6)	S(2)–C(5)	1.845(6)
P(1)–C(1)	1.827(5)	P(1)–C(7)	1.831(5)
P(1)–C(13)	1.832(5)	P(2)–C(6)	1.838(5)
P(2)–C(19)	1.817(6)	P(2)–C(25)	1.825(5)
C(1)–C(2)	1.520(7)	C(3)–C(4)	1.523(7)
C(5)–C(6)	1.493(8)		
Cl(1)–Ru–Cl(2)	94.17(4)	Cl(1)–Ru–S(1)	88.54(4)
Cl(1)–Ru–S(2)	177.37(5)	Cl(1)–Ru–P(1)	86.51(4)
Cl(1)–Ru–P(2)	93.26(5)	Cl(2)–Ru–S(1)	177.13(5)
Cl(2)–Ru–S(2)	88.12(4)	Cl(2)–Ru–P(1)	93.59(5)
Cl(2)–Ru–P(2)	86.87(5)	S(1)–Ru–S(2)	89.19(5)
S(1)–Ru–P(1)	85.62(5)	S(1)–Ru–P(2)	93.92(5)
S(2)–Ru–P(1)	94.65(5)	S(2)–Ru–P(2)	85.57(5)
P(1)–Ru–P(2)	179.50(5)	Ru–S(1)–C(2)	108.3(2)
Ru–S(1)–C(3)	104.2(2)	C(2)–S(1)–C(3)	98.3(3)
Ru–S(2)–C(4)	103.6(2)	Ru–S(2)–C(5)	108.2(2)
C(4)–S(2)–C(5)	99.3(3)	Ru–P(1)–C(1)	104.2(2)
Ru–P(1)–C(7)	123.8(2)	Ru–P(1)–C(13)	117.3(2)
C(1)–P(1)–C(7)	101.9(2)	C(1)–P(1)–C(13)	104.9(2)
C(7)–P(1)–C(13)	102.4(2)	Ru–P(2)–C(6)	104.5(2)
Ru–P(2)–C(19)	123.7(2)	Ru–P(2)–C(25)	117.7(2)
C(6)–P(2)–C(19)	102.9(2)	C(6)–P(2)–C(25)	105.1(3)
C(19)–P(2)–C(25)	100.8(2)	P(1)–C(1)–C(2)	110.5(3)
S(1)–C(2)–C(1)	110.2(4)	S(1)–C(3)–C(4)	111.6(4)
S(2)–C(4)–C(3)	112.0(4)	S(2)–C(5)–C(6)	111.1(4)
P(2)–C(6)–C(5)	110.8(4)		

---

[*] The ionic radius for Ru^{2+} is not given in ref. 8, however values for Ru^{3+} (0.68), Ru^{4+} (0.62) and Ru^{5+} (0.565 Å) are presented. Extrapolating these would give the ionic radius for Ru^{2+} as approximately 0.74 Å. Irrespective of this, since Ru^{3+} is larger than Rh^{3+}, it is clear that Ru^{2+} will be even larger.

observed for RSC_2H_4SR in this complex (*cis*-α) does not necessitate that two adjacent five-membered chelate rings lie parallel (*i.e.* there are no $PCH_2CH_2SCH_2CH_2S$ linkages occupying meridional co-ordination sites as would occur in the *cis*-β forms). This avoids the additional ring strain that would otherwise occur. The structure determined for $[RuCl_2(RSC_2H_4SR)]\cdot0.75Et_2O$ contrasts with that reported for $[RuCl_2\{RP(Ph)C_2H_4(Ph)PR\}]$ $[RP(Ph)C_2H_4(Ph)PR = Ph_2PCH_2CH_2P(Ph)CH_2CH_2(Ph)PCH_2CH_2PPh_2]$ in which a *trans*-dichloro stereochemistry is observed, with all three chelate rings occurring around the equatorial co-ordination sites.[14] It is likely that the high barrier to inversion at P and the steric effect of the Ph groups bound to the internal phosphines in $RP(Ph)C_2H_4(Ph)PR$ play a significant role in determining the stereochemistries of its complexes.

The stereochemistries of $[RuCl_2(RSC_2H_4SR)]$ and $[RuCl_2(Ph_2[14]aneP_2S_2)]$, although both involving *cis*-dichloro arrangements, are markedly different. This is mainly a consequence of the acyclic *vs.* macrocyclic configurations respectively. Clearly, unlike RSC_2H_4SR, it is not possible for $Ph_2[14]aneP_2S_2$ to co-ordinate to a metal ion to give a P-*trans*-P arrangement. Irrespective of this, $Ph_2[14]aneP_2S_2$ and RSC_2H_4SR each co-ordinates *via* all four donor atoms to give stable complexes. Unfortunately to date we have been unable to grow crystals of $[RuCl_2(Ph_2[14]aneP_2S_2)]$ suitable for a crystal structure determination.

We have also investigated the redox properties of the ruthenium(II) complexes by cyclic voltammetry. In CH_2Cl_2 solution (0.1 mol dm^{-3} $NBu^n{}_4BF_4$ supporting electrolyte) *cis*-$[RuCl_2(Ph_2[14]aneP_2S_2)]$ shows a reversible one-electron oxidation at $E_{\frac{1}{2}} = +0.32$ V *vs.* ferrocene–ferrocenium (Fig. 3), assigned to a Ru^{II}–Ru^{III} redox couple. This couple is observed at $E_{\frac{1}{2}} = +0.16$ V for *cis*-$[RuCl_2(RSC_2H_4SR)]$. These potentials are comparable with those for other dichlororuthenium(II) complexes involving phosphine and thioether ligands, *e.g.* $[RuCl_2(Ph_2PCH_2CH_2PPh_2)_2]^{0/+}$ ($E_{\frac{1}{2}} = +0.13$ V) and *trans*-$[RuCl_2(MeSCH_2CH_2SMe)_2]^{0/+}$ ($E_{\frac{1}{2}} = +0.14$ V).[15]

The related low-spin d^6 complexes $[MCl_2(RSC_2H_4SR)]PF_6$ (M = Rh or Ir) are obtained either by chloride abstraction from $[RhCl_3(RSC_2H_4SR)]$ (formed from $RhCl_3\cdot3H_2O$ and RSC_2H_4SR in EtOH–water), or by reaction of $[\{IrCl(C_8H_{14})_2\}_2]$ with 0.5 molar equivalents of RSC_2H_4SR followed by oxidation by Cl_2 and anion metathesis. The FAB mass spectra show highest-mass peaks with the correct isotopic patterns for $[RhCl_2(RSC_2H_4SR)]^+$ (m/z = 691) and $[IrCl_2(RSC_2H_4SR + H)]^+$ (m/z = 781), together with additional peaks corresponding to successive loss of Cl from these species. Proton NMR and IR spectroscopy and microanalytical data are also consistent with the formulation $[MCl_2(RSC_2H_4SR)]PF_6$ for these products.

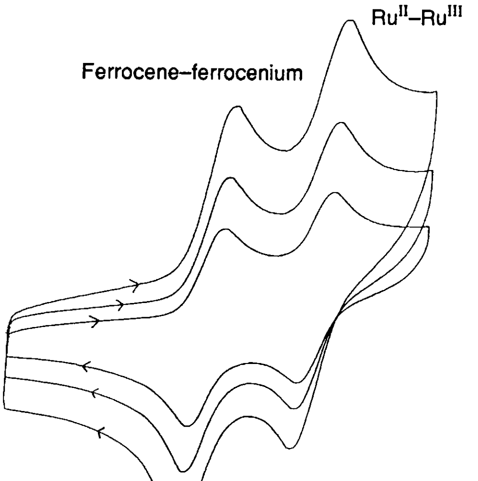

Fig. 3 Cyclic voltammogram of *cis*-$[RuCl_2(Ph_2[14]aneP_2S_2)]$ measured at 200, 100 and 50 mV s^{-1} in CH_2Cl_2 solution (0.1 mol dm^{-3} $NBu^n{}_4BF_4$ supporting electrolyte) and relative to equimolar ferrocene–ferrocenium

The single-crystal structure of $[RhCl_2(RSC_2H_4SR)]PF_6\cdot CH_2Cl_2$ shows (Fig. 4, Table 2) two independent half cations in which the Rh^{III} ions occupy sites of crystallographic two-fold symmetry, with one $PF_6{}^-$ anion in a general position in the asymmetric unit. The stereochemistry at Rh^{III} is very similar to that observed for $[RuCl_2(RSC_2H_4SR)]$ described above, with the cation showing a *cis*-α arrangement and similar trends in the metal–donor atom bond lengths and angles, Rh(1)–P(1) 2.352(2), Rh(1)–S(1) 2.303(2), Rh(1)–Cl(1) 2.370(2) Å, Rh(2)–P(2) 2.342(2), Rh(2)–S(2) 2.297(2), and Rh(2)–Cl(2)

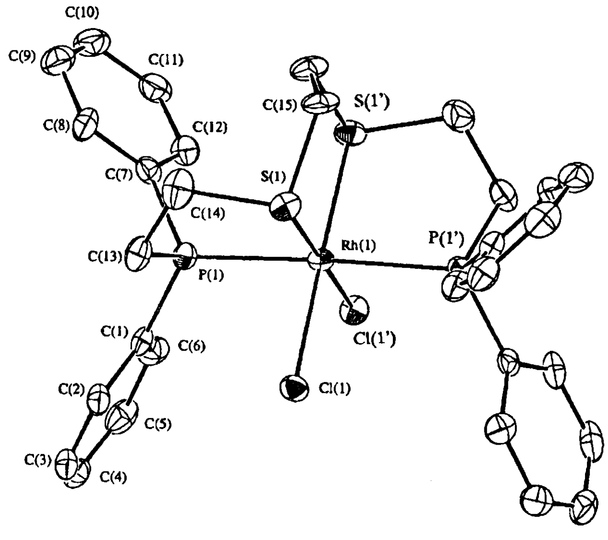

Fig. 4 View of the structure of one of the two independent *cis*-$[RhCl_2(RSC_2H_4SR)]^+$ cations with the numbering scheme adopted. Primed atoms are related to unprimed ones by a two-fold operation. The other cation is essentially indistinguishable; H atoms are omitted for clarity

Table 2 Selected bond lengths (Å) and angles (°) for *cis*-$[RhCl_2(RSC_2H_4SR)]^+$

Rh(1)–Cl(1)	2.370(2)	Rh(2)–Cl(2)	2.359(2)
Rh(1)–S(1)	2.303(2)	Rh(2)–S(2)	2.297(2)
Rh(1)–P(1)	2.352(2)	Rh(2)–P(2)	2.342(2)
S(1)–C(14)	1.839(7)	S(1)–C(15)	1.821(6)
S(2)–C(29)	1.832(7)	S(2)–C(30)	1.811(6)
P(1)–C(1)	1.819(6)	P(1)–C(7)	1.817(6)
P(1)–C(13)	1.818(6)	P(2)–C(16)	1.820(6)
P(2)–C(22)	1.806(6)	P(2)–C(28)	1.802(6)
C(13)–C(14)	1.533(9)	C(15)–C(15)	1.50(1)
C(28)–C(29)	1.523(9)	C(30)–C(30)	1.52(1)
Cl(1)–Rh(1)–Cl(1′)	92.74(8)	Cl(2)–Rh(2)–Cl(2′)	93.67(8)
Cl(1)–Rh(1)–S(1′)	177.53(6)	Cl(2)–Rh(2)–S(2)	88.11(5)
Cl(1)–Rh(1)–P(1′)	92.45(6)	Cl(2)–Rh(2)–P(2)	85.98(6)
Cl(1)–Rh(1)–S(1)	88.98(5)	Cl(2)–Rh(2)–S(2′)	177.50(6)
Cl(1)–Rh(1)–P(1)	85.51(6)	Cl(2)–Rh(2)–P(2′)	92.29(6)
S(1)–Rh(1)–P(1)	85.91(6)	S(2)–Rh(2)–S(2′)	90.15(9)
S(1)–Rh(1)–P(1′)	96.19(6)	S(2)–Rh(2)–P(2′)	95.70(6)
P(1)–Rh(1)–P(1′)	177.06(9)	S(2)–Rh(2)–P(2)	86.09(6)
S(1)–Rh(1)–S(1′)	89.36(8)	P(2)–Rh(2)–P(2′)	177.47(9)
Rh(1)–S(1)–C(14)	106.9(2)	Rh(1)–S(1)–C(15)	103.0(2)
C(14)–S(1)–C(15)	99.4(3)	Rh(2)–S(2)–C(29)	106.3(2)
Rh(2)–S(2)–C(30)	102.8(2)	C(29)–S(2)–C(30)	100.8(3)
Rh(1)–P(1)–C(1)	117.8(2)	Rh(1)–P(1)–C(7)	117.1(2)
Rh(1)–P(1)–C(13)	103.1(2)	C(1)–P(1)–C(7)	104.9(3)
C(1)–P(1)–C(13)	106.0(3)	C(7)–P(1)–C(13)	106.9(3)
Rh(2)–P(2)–C(16)	115.0(2)	Rh(2)–P(2)–C(22)	118.7(2)
Rh(2)–P(2)–C(28)	103.1(2)	C(16)–P(2)–C(22)	105.2(3)
C(16)–P(2)–C(28)	106.8(3)	C(22)–P(2)–C(28)	107.3(3)

2.359(2) Å. The ^{31}P-{^{1}H} NMR spectra of $[MCl_2(RSC_2H_4SR)]PF_6$ indicate that this stereochemistry and donor set is retained in solution, δ +41.1, $^{1}J_{RhP}$ = 85 Hz for M = Rh, δ +28.0 for M = Ir. The ^{103}Rh NMR spectrum (11.4 MHz) of *cis*-$[RhCl_2(RSC_2H_4SR)]PF_6$ shows a triplet at δ +1405 ($^{1}J_{RhP}$ = 85 Hz). This signal is intermediate between that observed for *trans*-$[RhCl_2(MeSCH_2CH_2SMe)_2]^+$ (δ 2502–2585, mixture of invertomers)[16] and *trans*-$[RhCl_2\{o\text{-}C_6H_4(PMe_2)_2\}_2]Cl$ (δ 628, qnt, $^{1}J_{RhP}$ 80 Hz).[17] It has already been noted that, for a given ligand set, changing from a *cis* to a *trans* arrangement results in a downfield shift, *e.g. cis*-$[RhCl_2(AsMe_3)_4]^+$ (δ 1455) and *trans*-$[RhCl_2(AsMe_3)_4]^+$ (δ 1946).[18]

The spectroscopic results obtained confirm that ligation of RSC_2H_4SR to the octahedral metal centres Ru^{II}, Rh^{III} or Ir^{III} yields a single isomeric form. Although low-temperature NMR spectra were not recorded, ligand exchange would not be expected in these low-spin d^6 compounds. The spectroscopic data are consistent with the *cis*-α arrangement observed in the solid state for Ru^{II} and Rh^{III} being retained in solution. The compound *meso*-$Ph_2[14]aneP_2S_2$, on the other hand, coordinates to Rh^{III} to give exclusively the *trans*-dichloro isomer, whereas the larger Ru^{II} is not compatible with the hole size available, and spectroscopic data indicate formation of the *cis*-dichloro isomer. We are currently investigating the possibility of chloride abstraction from these *cis*-dichloro species to yield substitution-labile co-ordination sites for uptake of for example N_2, O_2 or olefins.

Experimental

Infrared spectra were measured as KBr or CsI discs or as Nujol mulls using a Perkin-Elmer 983 spectrometer over the range 200–4000 cm^{-1}, solution UV/VIS spectra in quartz cells (1 cm path length) using a Perkin-Elmer Lambda19 spectrophotometer, mass spectra by electron impact (EI) or fast-atom bombardment (FAB) using 3-nitrobenzyl alcohol as matrix on a VG Analytical 70-250-SE normal-geometry double-focusing spectrometer, ^{1}H and ^{13}C-{^{1}H} NMR spectra using a Bruker AM300 spectrometer operating at 300 and 75.7 MHz respectively, and ^{31}P and ^{103}Rh NMR spectra in 10 mm NMR tubes containing 10–15% deuteriated solvent using a Bruker AM360 spectrometer operating at 145.8 and 11.4 MHz respectively and referenced to 85% H_3PO_4 (^{31}P, δ 0) and Ξ = 3.16 MHz (^{103}Rh, δ 0). Microanalyses were obtained from the Imperial College Microanalytical Laboratory. Cyclic voltammetric experiments were performed using an EG & G Princeton Applied Research model 362 scanning potentiostat with 0.1 mol dm^{-3} $NBu^n{}_4BF_4$ supporting electrolyte, using a double platinum electrode as working and auxiliary electrode and a Ag–AgCl reference electrode. All potentials are quoted *versus* ferrocene–ferrocenium. The compounds $[RuCl_2(py)_4]$[19] and PPh_2H[20] were prepared by the literature methods and $Ph_2[14]aneP_2S_2$ was obtained as described previously.[4]

(*a*) Synthesis of $[RuCl_2(Ph_2[14]aneP_2S_2)]$

To a solution of $[RuCl_2(py)_4]$ (56.0 mg, 0.11 mmol) in deoxygenated toluene was added $Ph_2[14]aneP_2S_2$ (47.1 mg, 0.11 mmol) under a flow of nitrogen. This reaction mixture was refluxed under a nitrogen atmosphere for 6 h before cooling. A yellow precipitate formed during the reaction and after cooling to −10 °C overnight this solid was filtered off and washed with diethyl ether. The product was recrystallised from CH_2Cl_2 and diethyl ether and dried *in vacuo* (37 mg, 56%) (Found: C, 41.2; H, 4.9. $C_{30}H_{32}Cl_2P_2RuS_2{\cdot}CH_2Cl_2$ requires C, 40.8; H, 4.7%). FAB mass spectrum: *m*/*z* = 557, 521 and 446; calc. 557 for $[^{102}Ru^{35}Cl(Ph_2[14]aneP_2S_2)]^+$, 522 for $[^{102}Ru(Ph_2[14]aneP_2S_2)]^+$ and 445 for $[^{102}Ru(Ph[14]aneP_2S_2)]^+$. NMR: ^{1}H (360 MHz, $CDCl_3$), δ 7.6–7.1 (m, 10 H, Ph) and 3.3–2.1 (m, 20 H, CH_2); ^{31}P-{^{1}H} (145.8 MHz, CH_2Cl_2–$CDCl_3$, 300 K), δ +63.5 (d, $^{2}J_{PP}$ 40) and 54.7 (d, $^{2}J_{PP}$ 40 Hz). UV/VIS (CH_2Cl_2): λ_{max} 330 (ε 1575 dm^3 mol^{-1} cm^{-1}) and 400 (sh) nm. IR (CsI disc): 3051w, 2917m, 1530w, 1184m, 1432vs, 1261m, 1102vs, 915w, 840w, 805m, 746m, 696vs, 486m, 309m and 283w cm^{-1}.

(*b*) Synthesis of RSC_2H_4SR

The compound PPh_2H (3.0 g, 16.1 mmol) was dissolved in dry, degassed thf (50 cm^3) and cooled to 0 °C. *n*-Butyllithium in hexane (19.3 mmol) was added dropwise over *ca.* 30 min to give a deep red solution which was then cooled to −78 °C (acetone slush). Ethylene sulfide $\overline{SCH_2C}H_2$ (0.96 cm^3, 16.1 mmol) dissolved in dry, degassed thf (20 cm^3) was then added over 2 h, followed by $BrCH_2CH_2Br$ (1.5 g, 8.06 mmol) dropwise to give a light yellow solution which was stirred under a nitrogen atmosphere overnight. After hydrolysing with water, the product was extracted with diethyl ether, dried ($MgSO_4$) and the solvent removed *in vacuo*. It was then recrystallised from CH_2Cl_2–EtOH to yield a white solid (3.57 g, 52%) (Found: C, 68.9; H, 6.2. $C_{30}H_{32}P_2S_2$ requires C, 69.5; H, 6.2%). FAB mass spectrum: *m*/*z* = 519; calc. 518 for RSC_2H_4SR. NMR: ^{1}H (300 MHz, $CDCl_3$), δ 7.5–7.3 (m, 20 H, Ph), 2.65 (m, 4 H, CH_2P), 2.55 (m, 4 H, SCH_2CH_2P), and 2.30 (m, 4 H, SCH_2CH_2S); ^{13}C-{^{1}H} (75.5 MHz, $CDCl_3$), δ 137.89 (quaternary C of Ph), 132.80, 129.01, 128.75 (CH of Ph), 31.12 (SCH_2CH_2S), 28.75 (PCH_2CH_2S), 28.70 (d, PCH_2, $^{2}J_{PC}$ = 37 Hz); ^{31}P (145.8 MHz, CH_2Cl_2–D_2O), δ −16.3. IR (CsI disc): 3066m, 3045w, 2941w, 2919m, 1583m, 1478vs, 1430vs, 1393w, 1326w, 1306w, 1280m, 1207m, 1178m, 1130w, 1097m, 1068m, 1025m, 998m, 907m, 843w, 757w, 737vs, 696vs, 531w, 504m, 479m, 438w and 395w cm^{-1}.

(*c*) Synthesis of *cis*-$[RuCl_2(RSC_2H_4SR)]$

To a refluxing solution of RSC_2H_4SR (50 mg, 0.097 mmol) in degassed toluene (35 cm^3) was added dropwise $[RuCl_2(py)_4]$ (47 mg, 0.097 mmol) dissolved in CH_2Cl_2–MeCN–toluene (1 : 1 : 2 v/v, 20 cm^3). After refluxing this orange solution for 12 h the solvent volume was reduced to *ca.* 5 cm^3. Addition of diethyl ether afforded the product as a yellow solid which was recrystallised from CH_2Cl_2–diethyl ether and dried *in vacuo* (57 mg, 82%) (Found: C, 48.2; H, 4.2. $C_{30}H_{32}Cl_2P_2RuS_2{\cdot}CH_2Cl_2$ requires C, 48.0; H, 3.8%). FAB mass spectrum: *m*/*z* = 690, 655 and 627; calc. 690 for $[^{102}Ru^{35}Cl_2(RSC_2H_4SR)]^+$, 655 for $[^{102}Ru^{35}Cl(RSC_2H_4SR)]^+$ and 627 for $[^{102}Ru^{35}Cl(RSC_2H_4SR - C_2H_4)]^+$. NMR ($CDCl_3$): ^{1}H (300 MHz), δ 7.5–7.3 (m, 20 H, Ph) and 3.3–1.8 (m, 12 H, CH_2); ^{31}P (145.8 MHz), δ + 42.7. UV/VIS (CH_2Cl_2): λ_{max} 254 (ε 24 000), *ca.* 360 (sh) (*ca.* 600) and 450nm (380 dm^3 mol^{-1} cm^{-1}). IR (CsI disc): 3050w, 2961w, 2917w, 1570w, 1482m, 1431vs, 1407m, 1314w, 1260m, 1189m, 1096vs, 1028m, 899w, 812m, 742m, 702vs, 662w, 517m, 495m and 270w cm^{-1}.

(*d*) Single-crystal structure determination on *cis*-$[RuCl_2(RSC_2H_4SR)]{\cdot}0.75Et_2O$

Orange prismatic crystals were obtained by vapour diffusion of Et_2O into a solution of the complex in CH_2Cl_2. The selected crystal (0.20 × 0.10 × 0.30 mm) was coated in silicone oil, mounted on a glass fibre and cooled under a stream of N_2 gas to prevent solvent loss.

Crystal data. $C_{33}H_{39.5}Cl_2O_{0.75}P_2RuS_2$ M = 746.2, monoclinic, space group $P2_1/n$, a = 13.080(5), b = 17.822(2), c = 15.003(1) Å, β = 102.87(2)°, U = 3409(1) Å^3 [from 2θ values of 25 reflections measured at ±ω (39.4 ⩽ 2θ ⩽ 39.9°, λ = 0.710 73 Å)], Z = 4, D_c = 1.454 g cm^{-3}, T = 123 K, μ = 0.857 mm^{-1}, F(000) = 1534.

Data collection and processing. Rigaku AFC7R four-circle diffractometer equipped with an Oxford Cryostreams low-

Table 3 Fractional atomic coordinates for *cis*-[$RuCl_2(RSC_2H_4SR)$]$\cdot$0.75Et_2O

Atom	*x*	*y*	*z*	Atom	*x*	*y*	*z*
Ru	0.516 38(3)	0.042 58(2)	0.751 89(3)	C(14)	0.798 1(4)	−0.121 5(3)	0.846 4(4)
Cl(1)	0.510 81(9)	0.143 19(7)	0.863 22(8)	C(15)	0.852 2(4)	−0.176 0(3)	0.808 9(4)
Cl(2)	0.581 51(10)	0.125 18(7)	0.645 11(8)	C(16)	0.865 5(4)	−0.168 8(3)	0.721 6(4)
S(1)	0.458 6(1)	−0.039 40(7)	0.847 82(9)	C(17)	0.824 5(4)	−0.106 6(3)	0.670 4(4)
S(2)	0.515 3(1)	−0.053 69(7)	0.650 41(9)	C(18)	0.771 7(4)	−0.051 7(3)	0.706 6(4)
P(1)	0.684 5(1)	0.015 88(8)	0.838 13(9)	C(19)	0.300 6(4)	0.163 2(3)	0.634 7(4)
P(2)	0.347 9(1)	0.068 96(8)	0.666 89(9)	C(20)	0.362 3(5)	0.225 7(3)	0.661 3(4)
O	0.850 9(7)	0.173 2(6)	0.513 8(5)	C(21)	0.323 3(6)	0.297 5(4)	0.632 0(5)
C(1)	0.662 2(4)	−0.019 3(3)	0.946 6(3)	C(22)	0.226 2(6)	0.305 2(4)	0.574 7(5)
C(2)	0.574 0(4)	−0.076 7(3)	0.929 9(3)	C(23)	0.163 5(6)	0.242 4(4)	0.547 9(4)
C(3)	0.424 0(4)	−0.123 7(3)	0.779 0(4)	C(24)	0.200 6(5)	0.172 2(4)	0.578 8(4)
C(4)	0.499 1(4)	−0.137 2(3)	0.716 2(4)	C(25)	0.237 2(4)	0.030 5(3)	0.707 4(4)
C(5)	0.387 1(4)	−0.053 7(3)	0.568 5(4)	C(26)	0.222 3(4)	0.057 9(4)	0.790 1(4)
C(6)	0.341 9(4)	0.023 5(3)	0.555 9(3)	C(27)	0.136 7(5)	0.033 9(4)	0.823 8(4)
C(7)	0.785 5(4)	0.087 2(3)	0.876 5(3)	C(28)	0.066 1(5)	−0.017 8(4)	0.775 4(5)
C(8)	0.879 7(4)	0.067 2(3)	0.936 1(4)	C(29)	0.082 7(5)	−0.046 6(4)	0.694 6(5)
C(9)	0.953 8(4)	0.121 0(3)	0.970 6(4)	C(30)	0.167 0(5)	−0.021 8(4)	0.659 4(4)
C(10)	0.936 8(4)	0.195 7(3)	0.944 8(4)	C(31)	0.941 5(8)	0.163 8(8)	0.672 9(7)
C(11)	0.845 5(4)	0.215 9(3)	0.883 4(4)	C(32)	0.878(1)	0.127(1)	0.601 8(10)
C(12)	0.769 0(4)	0.161 8(3)	0.849 1(4)	C(33)	0.771(1)	0.236 4(8)	0.476(1)
C(13)	0.758 0(4)	−0.058 7(3)	0.796 2(4)	C(34)	0.779(1)	0.241 5(9)	0.391(1)

temperature attachment, using graphite-monochromated Mo-Kα X-radiation, ω scans with ω-scan width = (1.68 + 0.35 tan θ)°, 8040 data collected, 7710 unique (R_{int} = 0.016) ($2\theta_{max}$ 54°, *h* 0–22, *k* −18 to 18, *l* −18 to 17) giving 6511 reflections with $F \geqslant 5\sigma(F)$ for use in all calculations. No significant crystal decay or movement was observed. The data were corrected for Lorentz and polarisation effects. No absorption correction was applied since preliminary ψ scans revealed no significant absorption.

Structure solution and refinement. The structure was solved by direct methods[21] and developed by using iterative cycles of full-matrix least-squares refinement and Fourier-difference syntheses which located all non-H atoms in an ordered [$RuCl_2(RSC_2H_4SR)$] molecule.[22] During refinement a partially occupied (75%) Et_2O solvent molecule was found to be present. All non-H atoms were refined anisotropically, while H atoms were located in the difference map and their coordinates fixed. The weighting scheme $w^{-1} = \sigma^2(F)$ gave satisfactory agreement analyses. At final convergence *R*, *R'* = 0.043, 0.068 respectively, *S* = 5.59 for 380 refined parameters. The final ΔF synthesis showed no peaks above 1.31 or below −0.88 e Å^{-3} and the maximum Δ/σ = 0.01. Fractional atomic coordinates are listed in Table 3.

(*e*) Synthesis of *cis*-[$RhCl_2(RSC_2H_4SR)$]PF_6

The phosphine (0.0986 g, 0.190 mmol) was dissolved in degassed ethanol (15 cm^3) and heated to reflux; $RhCl_3\cdot3H_2O$ (50 mg, 0.19 mmol) was dissolved in water–ethanol (1 : 2 v/v, 15 cm^3) and added dropwise over 1 h. Reflux was continued for 1.5 h before the resulting orange solution was allowed to cool. A small amount of yellow ethanol-insoluble solid was filtered off. The solvent was then removed *in vacuo* and the product redissolved in CH_2Cl_2 and filtered once again. The product, thought to be $RhCl_3(RSC_2H_4SR)$, was precipitated as a pale orange solid by the addition of diethyl ether (116 mg, 84%). This was dissolved in MeCN–CH_2Cl_2 (1 : 1 v/v, 30 cm^3) and refluxed for 1 h with $TlPF_6$ (56 mg, 0.16 mmol). The resulting yellow-orange solution was filtered through Celite to remove the white TlCl precipitated. The product was precipitated from CH_2Cl_2–diethyl ether as a yellow powder and dried *in vacuo* (76 mg, 48%) (Found: C, 39.5; H, 3.9. $C_{30}H_{32}Cl_2F_6P_3RhS_2\cdot CH_2Cl_2$ requires C, 40.4; H, 3.7%). FAB mass spectrum: *m*/*z* = 691, 656 and 621; calc. 691 for [$^{103}Rh^{35}Cl_2(RSC_2H_4SR)$]$^+$, 656 for [$^{103}Rh^{35}Cl(RSC_2H_4SR)$]$^+$ and 621 for [$^{103}Rh(RSC_2H_4SR)$]$^+$. NMR: ^1H (300 MHz, $CDCl_3$), δ 7.9–7.3 (m, 20 H, Ph) and 3.5–2.6 (m, 12 H, CH_2); ^{31}P (145.8 MHz, CH_2Cl_2–D_2O), δ +41.1 (d, 2 P, $^1J_{RhP}$ = 85, RSC_2H_4SR) and −146.3 (spt, 1 P, PF_6^-); ^{103}Rh (11.4 MHz, MeCN–CD_3CN, 300 K), δ +1405 (t, 85 Hz). UV/VIS (MeCN): λ_{max} 226 (sh) (ε *ca.* 33 000), 286 (sh) (*ca.* 18 500), 316 (23 000) and 421 (sh) nm (*ca.* 550 dm^3 mol^{-1} cm^{-1}). IR (CsI disc): 3060w, 2963w, 1570w, 1482m, 1433vs, 1406m, 1337w, 1314w, 1262w, 1191w, 1097m, 1027m, 998w, 840vs, 745m, 709m, 694m, 558vs, 520m, 368w and 336w cm^{-1}.

(*f*) Single-crystal structure determination on *cis*-[$RhCl_2(RSC_2H_4SR)$]$PF_6\cdot CH_2Cl_2$

Orange rhomb-shaped crystals were obtained by vapour diffusion of Et_2O into a solution of the complex in CH_2Cl_2. The selected crystal (0.60 × 0.44 × 0.26 mm) was coated in silicone oil, mounted on a glass fibre and cooled under a stream of N_2.

Crystal data. $C_{31}H_{34}Cl_4P_2RhS_2{}^+\cdot PF_6{}^-$, *M* = 922.4, monoclinic, space group *C*2/*c*, *a* = 25.183(5), *b* = 15.622(5), *c* = 22.520(5) Å, β = 123.90(1)°, *U* = 7352(3) Å^3 [from 2θ values of 23 reflections measured at $\pm\omega$ ($39.0 \leqslant 2\theta \leqslant 39.9$°, λ = 0.710 73 Å)], *Z* = 8, D_c = 1.666 g cm^{-3}, *T* = 123 K, μ = 1.052 mm^{-1}, *F*(000) = 3712.

Data collection and processing. As for [$RuCl_2(RSC_2H_4SR)$] except ω scan width = (1.78 + 0.35 tan θ)°, 6157 data collected, 6004 unique (R_{int} = 0.051) ($2\theta_{max}$ 48°, *h* 0–32, *k* 0–20, *l* −29 to 29) giving 4248 reflections with $F \geqslant 5\sigma(F)$ for use in all calculations.

Structure solution and refinement. Structure solution as for [$RuCl_2(RSC_2H_4SR)$] located all non-H atoms in the two independent half [$RhCl_2(RSC_2H_4SR)$]$^+$ cations, one complete $PF_6{}^-$ anion and CH_2Cl_2 solvent molecule in the asymmetric unit.[22] Since there were no identifiable faces on the crystal, at isotropic convergence the data were corrected for absorption using DIFABS[23] (maximum and minimum transmission factors = 1.174 and 0.868 respectively). All non-H atoms were refined anisotropically, while H atoms were placed in fixed, calculated positions. The weighting scheme $w^{-1} = \sigma^2(F)$ gave satisfactory agreement analyses. At final convergence *R*, *R'* = 0.045, 0.043 respectively, *S* = 3.55 for 425 refined parameters.

Table 4 Fractional atomic coordinates for *cis*-$[RhCl_2(RSC_2H_4SR)]PF_6 \cdot CH_2Cl_2$

Atom	*x*	*y*	*z*	Atom	*x*	*y*	*z*
Rh(1)	0	−0.777 23(4)	−0.25	C(8)	−0.058 0(3)	−0.658 7(3)	−0.469 1(3)
Rh(2)	0	−0.280 72(4)	−0.25	C(9)	−0.031 8(4)	−0.613 7(4)	−0.500 1(4)
Cl(1)	−0.074 93(7)	−0.881 90(9)	−0.265 69(9)	C(10)	0.030 8(4)	−0.628 3(4)	−0.478 0(4)
Cl(2)	−0.039 32(8)	−0.384 02(10)	−0.341 65(9)	C(11)	0.067 6(3)	−0.686 4(4)	−0.423 7(4)
Cl(3)	0.206 8(1)	0.188 1(3)	−0.288 1(2)	C(12)	0.042 6(3)	−0.729 3(4)	−0.390 7(3)
Cl(4)	0.253 3(1)	0.244 2(2)	−0.142 9(2)	C(13)	−0.132 1(3)	−0.736 1(4)	−0.405 8(3)
S(1)	−0.072 08(8)	−0.672 39(10)	−0.268 55(9)	C(14)	−0.122 9(3)	−0.652 6(4)	−0.365 5(4)
S(2)	−0.040 07(8)	−0.176 89(10)	−0.336 89(9)	C(15)	−0.023 8(3)	−0.575 3(4)	−0.240 1(4)
P(1)	−0.054 28(8)	−0.781 1(1)	−0.375 28(8)	C(16)	−0.112 9(3)	−0.214 2(4)	−0.213 9(3)
P(2)	−0.102 20(8)	−0.284 0(1)	−0.271 11(9)	C(17)	−0.158 4(3)	−0.150 2(4)	−0.240 9(4)
P(3)	0.291 82(9)	−0.022 1(1)	−0.048 3(1)	C(18)	−0.163 1(4)	−0.096 9(4)	−0.194 3(5)
F(1)	0.316 9(2)	0.033 2(4)	−0.085 7(3)	C(19)	−0.124 7(4)	−0.110 1(5)	−0.122 1(5)
F(2)	0.299 3(3)	−0.104 0(4)	−0.084 0(4)	C(20)	−0.080 1(4)	−0.174 9(5)	−0.095 0(4)
F(3)	0.267 4(2)	−0.082 6(4)	−0.012 2(3)	C(21)	−0.072 4(3)	−0.225 4(4)	−0.139 8(3)
F(4)	0.282 7(2)	0.059 7(4)	−0.014 5(3)	C(22)	−0.135 1(3)	−0.386 0(4)	−0.269 3(3)
F(5)	0.220 1(2)	−0.011 5(3)	−0.115 2(2)	C(23)	−0.115 1(3)	−0.424 6(4)	−0.204 3(4)
F(6)	0.363 1(2)	−0.029 0(3)	−0.017 8(3)	C(24)	−0.138 6(4)	−0.503 2(4)	−0.200 6(4)
C(1)	−0.070 0(3)	−0.885 3(4)	−0.418 0(3)	C(25)	−0.183 4(3)	−0.544 5(4)	−0.262 9(4)
C(2)	−0.130 2(3)	−0.923 6(4)	−0.451 5(3)	C(26)	−0.204 7(3)	−0.507 4(4)	−0.328 0(4)
C(3)	−0.141 6(3)	−1.002 3(4)	−0.484 2(4)	C(27)	−0.179 7(3)	−0.429 7(4)	−0.331 3(4)
C(4)	−0.093 3(4)	−1.045 2(4)	−0.483 7(4)	C(28)	−0.152 6(3)	−0.242 6(4)	−0.360 8(3)
C(5)	−0.032 8(3)	−1.008 4(4)	−0.448 9(4)	C(29)	−0.123 5(3)	−0.160 2(5)	−0.366 6(4)
C(6)	−0.021 5(3)	−0.929 2(4)	−0.417 1(4)	C(30)	−0.003 4(3)	−0.080 1(4)	−0.285 8(3)
C(7)	−0.021 5(3)	−0.717 0(4)	−0.415 0(3)	C(31)	0.234 4(5)	0.156 6(7)	−0.202 9(6)

The final ΔF synthesis showed no peaks above 1.43 or below -1.02 e Å^{-3} and the maximum $\Delta/\sigma = 0.01$. Fractional atomic coordinates are listed in Table 4.

Complete atomic coordinates, thermal parameters and bond lengths and angles for both crystal structures have been deposited at the Cambridge Crystallographic Data Centre. See Instructions for Authors, *J. Chem. Soc., Dalton Trans.*, 1996, Issue 1.

(*g*) Synthesis of $[IrCl_2(RSC_2H_4SR)]PF_6$

The complex $[\{IrCl(C_8H_{14})_2\}_2]$ (98 mg, 0.145 mmol) and RSC_2H_4SR (150 mg, 0.289 mmol) were added to degassed methanol (40 cm^3) giving a yellow solution, which was refluxed overnight under N_2. On cooling to 0 °C a solution of Cl_2 in CCl_4 was added (≈ 5 cm^3), causing the colour to fade. After stirring for 10 min the solvent was removed *in vacuo*. The resulting solid was refluxed in water (80 cm^3), NH_4PF_6 (100 mg) was added in MeCN and reflux was continued overnight. Removal of the solvent *in vacuo* and precipitation from CH_2Cl_2 by addition of Et_2O gave a pale yellow solid (147 mg, 45%). (Found: C, 38.8; H, 3.5. $C_{30}H_{32}Cl_2F_6IrP_3S_2$ requires C, 38.9; H, 3.5%). FAB mass spectrum: m/z = 781, 747 and 683; calc. 780 for $[^{192}Ir^{35}Cl_2(RSC_2H_4SR)]^+$, 745 for $[^{192}Ir^{35}Cl(RSC_2H_4SR)]^+$ and 682 for $[^{192}Ir(RSC_2H_4SR - C_2H_4]^+$. NMR: ^1H (300 MHz, $CDCl_3$); δ 7.8–7.1 (m, 20 H, Ph) and 3.4–2.2 (m, 12 H, CH_2); ^{31}P (145.8 MHz, CH_2Cl_2–$CDCl_3$) δ +28.0 (2P, RSC_2H_4SR) and −146.3 (spt, 1P, PF_6^-). IR (CsI disc): 3053w, 2963w, 2920w, 1570w, 1482m, 1432vs, 1405w, 1311w, 1272w, 1162w, 1099m, 1027w, 998w, 840vs, 744m, 695m, 558vs, 537m, 526m, 494w and 375w cm^{-1}.

Acknowledgements

We thank the EPSRC and the University of Southampton for support and Johnson Matthey plc for generous loans of platinum metal salts.

References

1 *The Chemistry of Organophosphorus Compounds*, ed. F. R. Hartley, Wiley, New York, 1990, vol. 1.

2 S. G. Murray and F. R. Hartley, *Chem. Rev.*, 1981, **81**, 365.

3 A. J. Blake and M. Schröder, *Adv. Inorg. Chem.*, 1990, **35**, 1; S. R. Cooper and S. C. Rawle, *Struct. Bonding (Berlin)*, 1990, **72**, 1.

4 N. R. Champness, C. S. Frampton, G. Reid and D. A. Tocher, *J. Chem. Soc., Dalton Trans.*, 1994, 3031.

5 C. L. Doel, C. S. Frampton, A. M. Gibson and G. Reid, *Polyhedron*, 1995, **14**, 3139.

6 A. M. Gibson and G. Reid, *J. Chem. Soc., Dalton Trans.*, 1996, following paper.

7 P. Garrou, *Chem. Rev.*, 1981, **81**, 229.

8 R. D. Shannon, *Acta Crystallogr. Sect. A*, 1976, 751.

9 A. J. Blake, G. Reid and M. Schröder, *J. Chem. Soc., Dalton Trans.*, 1989, 1675.

10 A. J. Blake, R. O. Gould, G. Reid and M. Schröder, *J. Organomet. Chem.*, 1988, **356**, 389.

11 T.-F. Lai and C.-K. Poon, *J. Chem. Soc., Dalton Trans.*, 1982, 1465.

12 Y.-M. Hsiao, S. S. Chojnacki, P. Hinton, J. H. Reibenspies and M. Y. Darensbourg, *Organometallics*, 1993, **12**, 870.

13 See D. A. House, in *Comprehensive Coordination Chemistry*, eds. R. D. Gillard, J. A. McCleverty and G. A. Wilkinson, Pergamon, Oxford, 1987, vol. 2.

14 A. V. Rivera, E. R. De Gil and B. Fontal, *Inorg. Chim. Acta*, 1985, **98**, 153.

15 N. R. Champness, W. Levason, D. Pletcher and M. Webster, *J. Chem. Soc., Dalton Trans.*, 1992, 3243.

16 H. C. E. McFarlane, W. McFarlane and R. J. Wood, *Bull. Soc. Chim. Belg.*, 1976, **85**, 864.

17 S. R. Preece, Ph. D. Thesis, University of Southampton, 1995.

18 See B. E. Mann, in *Transition Metal Nuclear Magnetic Resonance*, ed. P. S. Pregosin, Elsevier, Amsterdam, 1991.

19 I. P. Evans, A. Spencer and G. Wilkinson, *J. Chem. Soc., Dalton Trans.*, 1973, 204; 1770.

20 V. D. Bianco and S. Doronzo, *Inorg. Synth.*, 1976, **16**, 161.

21 SHELXS 86, program for crystal structure solution, G. M. Sheldrick, *Acta Crystallogr., Sect. A*, 1990, **46**, 467.

22 TEXSAN Crystal Structure Analysis Package, Molecular Structure Corporation, Houston, TX, 1992.

23 DIFABS, An Empirical Absorption Correction Program, N. Walker and D. Stuart, *Acta Crystallogr., Sect. A*, 1983, **39**, 158.

Received 9th October 1995; *Paper* 5/06628J